Integrative Biology

PAPER

Ligand density elicits a phenotypic switch in human neutrophils†

Cite this: *Integr. Biol.*, 2014, 6, 348

Steven J. Henry,[a] John C. Crocker[b] and Daniel A. Hammer*[ab]

Received 28th October 2013,
Accepted 5th January 2014

DOI: 10.1039/c3ib40225h

www.rsc.org/ibiology

Neutrophils are mediators of innate immunity and motility is critical to their function. We used microcontact printing to investigate the relationship between density of adhesive ligands and the dynamics of neutrophil motility. We show that neutrophils adopt a well-spread morphology without a uropod on moderate densities of adhesion ligand. As density is increased, the morphology switches to a classic amoeboid shape. In addition to the morphological differences, the dynamics of motility were quantitatively distinct. Well-spread cells without uropods glide slowly with high persistence, while amoeboid cells made frequent directional changes migrating quickly with low persistence. Using an antibody panel against various integrin chains, we show that adhesion and motility on fibronectin are mediated by MAC-1 ($\alpha_M\beta_2$). The phenotypic switch could be generalized to other surface ligands, such as bovine serum albumin, to which the promiscuous MAC-1 also binds. These results suggest that neutrophils are capable of displaying multiple modes of motility as dictated by their adhesive environment.

Insight, innovation, integration

There is substantial appreciation for the role soluble factors play in orchestrating immunologic surveillance, but relatively little appreciation of how adhesion controls leukocyte migration. In this study, we demonstrate the capacity of a highly motile immunologic cell, the neutrophil, to adhere and migrate on fields of adhesive ligand in a density-dependent manner. We observe a phenotypic switch in cell morphology as a function of surface adhesivity. The principle tool we employed was microcontact printing to immobilize fields of adhesive ligand. Our work contributes to a growing body of evidence that motile cells to achieve translocation by employing multiple migratory mechanisms.

Introduction

Leukocytes are important mediators of immunity, and motility is critical to their function. Neutrophils, in particular, act as first responders to pathogenic challenges[1] as well as sterile trauma[2] resulting in inflammation. The role of soluble chemoattractants in stimulating and directing neutrophil motility has long been of interest[1] and explored in various engineered *in vitro* systems.[3] Recently, attention has shifted to how the dimensionality of the environment controls leukocyte migration.[4] As the empirical body of leukocyte observations has grown, it is now appreciated that these cells can employ an assortment of migratory mechanisms.

On a majority of two-dimensional *in vitro* substrates, neutrophils exhibit an amoeboid morphology.[3,5] The distinguishing features of this phenotype are an elongated cell body with a frontward ruffled-lamellipodium, a midregion that contains the nucleus, and rearward knob-like uropod.[5a] Detailed images of this morphology have been captured with high resolution scanning electron microscopy (SEM).[6] However, there have also been observations of neutrophils assuming a very different, well-spread phenotype without uropods on two-dimensional substrates.[7] In those instances the alternative phenotype was attributed to the underlying stiffness of the material, as neutrophils on softer substrates were shown to re-assume an amoeboid phenotype. Yet, neutrophils also display the amoeboid phenotype on stiff substrates, such as those in the previously cited SEM studies, suggesting substrate stiffness is not a unique controller of cell morphology.[8] Hypothesizing that another factor was involved in modulating these two phenotypes, our study focused on the role of ligand density.

We investigated neutrophil morphology and motility on increasing densities of the extracellular matrix protein fibronectin (FN). We observed that neutrophils exhibited a well-spread, uropod-absent phenotype on sub-saturating, intermediate densities of FN. On high densities of ligand this phenotype was

[a] *Department of Bioengineering, University of Pennsylvania, 210 S 33rd St, Philadelphia, PA 19104, USA*
[b] *Department of Chemical and Biomolecular Engineering, University of Pennsylvania, 220 S 33rd St, Philadelphia, PA 19104, USA.*
E-mail: hammer@seas.upenn.edu

† Electronic supplementary information (ESI) available: Movie S1, Movie S2, and a PDF containing Fig. S1–S7 and associated text. See DOI: 10.1039/c3ib40225h

replaced with the amoeboid phenotype. The modes of motility associated with these two morphologies were quantifiably distinct as shown by comparison of their mean squared displacements with time. Finally, we determined that the FN adhesion and motility were mediated by MAC-1 ($\alpha_M\beta_2$). The phenotypic switch could be generalized to other surface ligands, such as bovine serum albumin, to which the promiscuous MAC-1 also binds.

Materials and methods

Media

Rinsing buffer was Hanks' Balanced Salt Solution (Invitrogen, Carlsbad, CA) without calcium or magnesium supplemented with 10 mM HEPES (Invitrogen) and pH adjusted to 7.4. Storage buffer was rinsing buffer supplemented with 2 mg mL^{-1} glucose. Running buffer was storage buffer supplemented with 1.5 mM Ca^{2+} and 2 mM Mg^{2+}. Fibronectin (FN) was from human plasma (BD Biosciences, Bedford, MA). Low-endotoxin bovine serum albumin (BSA) (Sigma) was prepared at 2% and 0.2% w/v in PBS without calcium and magnesium (PBS(−)). Labeling of proteins *via* Alexa Fluor carboxylic acid, succinimidyl ester (Invitrogen) was performed in accordance with the manufacturer's recommended protocol. Stock *N*-formylmethionyl-leucyl-phenylalanine (fMLF) (Sigma, Saint Louis, MO) was reconstituted in glacial acetic acid before dilution. The nonionic triblock copolymer Pluronic F-127 (Sigma) was prepared at 0.2% w/v in PBS(−). All solutions were sterile filtered or prepared sterile. Bicinchoninic acid protein assays (Pierce Biotechnology, Rockford, Il) were performed on stock solutions of proteins to measure concentration.

Substrates

Poly(dimethylsiloxane) (PDMS) (Sylgard 184 Silicone Elastomer, Dow Corning, Midland, MI) coated coverslips were prepared from number one thickness glass coverslips (Fisher Scientific, Hampton, NH) of 25 mm diameter spun with degassed PDMS (10 : 1 base : cure by weight). Spinning at 4000 rpm for 1 min, leveling at RT, and baking at 65 °C overnight resulted in a 12.5 ± 0.4 μm layer of PDMS. Bare glass coverslips were cleaned *via* piranha wash (2 : 1 by volume H_2SO_4 : H_2O_2) and thoroughly rinsed in diH_2O. Coverslips were dried completely in a 90 °C oven. Coverslips, bare and PDMS-coated, were affixed to the bottom of six-well tissue culture plates which had either been hot-punched or laser-cut to generate a 22 mm diameter opening in the bottom of the wells. Coverslip bonding was performed using a continuous bead of Norland Optical Adhesive 68 (Thorlabs, Newton, NJ), cured for 20 min under a long wavelength ultraviolet lamp.

Protein deposition and blocking

Stamps for printing were prepared from PDMS, mixed at 10 : 1 base : cure by weight, degassed, and poured over a silicon wafer. The polymer was cured by baking for 2 h or longer at 90 °C. Trimmed stamps were sonicated in 200 proof ethanol for 10 min, rinsed twice in diH_2O and dried in a gentle stream of filtered N_2(g). The face of the PDMS stamp previously cast against the silicon wafer was covered with a sessile drop of protein solution. After incubation, stamps were rinsed twice in a submerging quantity (~50 mL) of diH_2O and dried in a gentle stream of filtered N_2(g). For motility studies stamps were 1 cm^2, inked with 200 μL of protein solution for 2 h at RT. For all other experiments, stamps were 0.36 cm^2, inked with 50 μL of protein solution for 1 h at RT. After stamp inking and drying, mounted PDMS-coated coverslips were treated for 7 min with ultraviolet ozone (UVO Cleaner Model 342, Jelight, Irvine, CA) to render the surface hydrophilic.[9] Stamps were placed in conformal contact with the activated substrate for approximately 30 s.

For physisorption experiments, sterile flexiPERM (Sigma) silicone gaskets were affixed to the substrates to hold an aliquot of protein at a concentration and volume that preserved the number of protein molecules per unit area of exposed surface for comparison with the printed conditions.

Blocking printed or adsorbed surfaces by submersion in 0.2% w/v solutions of Pluronic F-127 or BSA (0.2% or 2%) was performed for 1 h. Native glass is not amenable to Pluronic blocking until silanized by immersion in 5% dimethyl dichlorosilane (Sigma) in dicholorobenzene (Sigma).[10] After blocking, each well was rinsed four or five times with 2 mL PBS(−) without dewetting the functionalized surface to prevent Pluronic sloughing. If substrates were not used the day of fabrication, they were stored overnight at 4 °C under PBS(−). Prior to cell plating, storage PBS(−) was exchanged for running buffer, without dewetting, and equilibrated to 37 °C at 5% CO_2 in a cabinet incubator.

Neutrophil isolation

Whole blood was obtained from human donors *via* venipuncture and collection in heparin vials. Samples were collected with University of Pennsylvania Institutional Review Board approval from consenting adult volunteers. Volunteers were required to be in good health and abstain from alcohol and all over-the-counter medication for 24–48 h prior to donation. Blood samples were allowed to cool to RT (15–30 min) and layered in a 1 : 1 ratio of whole blood to Polymorphprep (Axis-Shield, Oslo, Norway). Vials were spun for 45 min at 500 × *g* and 21 °C. After separation, the polymorphonuclear band and underlying separation media layer were aspirated into fresh round-bottom tubes. The isolated solution of cells and separation-media was diluted with rinsing buffer and spun for 5 min at 350 × *g* and 21 °C. Red Blood Cells (RBC) were eliminated from the resulting cell pellet *via* hypotonic lysis. After lysis, vials were centrifuged for 5 min at 350 × *g* and 21 °C and the RBC-free pellets resuspended in storage buffer. Neutrophils were stored at a concentration less than or equal to 1 × 10^6 cells mL^{-1} on a tube rotisserie at 4 °C until time of plating.

Cell motility experiments

For a given experimental condition, 7.5 × 10^4 neutrophils were seeded on a pre-equilibrated substrate under 1.5 mL of running buffer. Visual confirmation was made that cells had a rounded

(*i.e.* not polarized) morphology at time of plating. Substrates and cells were incubated 10 min at 37 °C and 5% CO_2 to allow settling and gently rinsed twice with 1 mL of fresh running buffer to remove non-adherent cells. Prior to rinsing, visual observation of the cells confirmed a transition from rounded to a well-spread morphology. Cell density was minimized to prevent cell–cell collisions but sufficiently dense to acquire reasonable sample sizes for statistical testing. Adherent neutrophils at multiple locations on the same substrate were imaged by time-lapse videomicroscopy for 30 min or longer at 30–90 s intervals in a temperature controlled chamber.

Phase-contrast image stacks corresponding to each imaging location of a particular experimental condition were processed *via* a custom MATLAB (The MathWorks, Natick, MA) script that identified cell boundaries, computed geometric centroids, and connected centroids in consecutive frames to form trajectories. Portions of trajectories were only retained for cells prior to cell–cell collisions and for cells that did not undergo apoptosis. To improve statistical power, multiple locations were imaged per condition. Summing across all field of views (FOVs) acquired we observed a total of 2688 neutrophils, 60% of which (n = 1606) where tracked and their trajectories utilized in MSD construction and curve fitting. Within this group of observed and tracked cells 75% (n = 1204) were tracked for 30 min and used in model-independent analyses. The remaining cells were tracked for only a portion of that observation window as they subsequently underwent cell–cell collisions. Of those cells that were observed but not tracked (n = 1082), 88% were excluded on the basis of cell–cell contact, residing at the edge of the FOV, or exiting the FOV. The remaining 12% were excluded on the basis of having an anomalous phenotype (*e.g.* appearing apoptotic). Cell tracking, mean-squared displacement computation, and error analysis were based upon the multiple particle tracking method reviewed by Crocker and Hoffman.[11]

Integrin blocking

The following panel of function-blocking antibodies against various integrin chains was assembled and used at final concentrations of 50 μg mL^{-1}: anti-β_1 clone MAb13 (BD Biosciences), anti-β_2 clone L130 (BD Biosciences), anti-α_M clone ICRF44 (eBioscience), and anti-α_5 clone SAM1 (eBioscience). Isotype controls to IgG1 and IgG2a were purchased from eBioscience. 5×10^5 neutrophils in 200 μL running buffer were incubated for 10 min with antibodies at RT with periodic mixing before exposure to the FN substrate. Substrates and cells were incubated 10 min at 37 °C and 5% CO_2 and immediately fixed in a solution of 4% formaldehyde (Fisher) or 10% neutral buffered formalin (Sigma) for 30 min at RT with periodic mixing. After fixation substrates were rinsed thoroughly with PBS to remove nonadherent cells.

Results and discussion

Observation of distinct neutrophil phenotypes on two different substrates

A common method of preparing two-dimensional surfaces for motility is to adsorb an adhesive ligand onto glass or polystyrene and subsequently wash with a solution of bovine serum albumin (BSA). The BSA wash is intended to mask bare regions of the substrate, unoccupied by protein, and impede non-specific cell–substrate interactions. When we plated human neutrophils on such a surface (fibronectin (FN)-adsorbed and BSA-blocked) the cells assumed an amoeboid phenotype having elongated cell bodies, trailing uropods, and narrow lamellipodia (Fig. 1a). The associated motility was undular, with cells undergoing frequent directional changes (Movie S1, ESI†). The amoeboid phenotype has been reported elsewhere[3,5,6] for neutrophils on various two-dimensional surfaces. By contrast, when we printed a poly(dimethylsiloxane) (PDMS) surface with FN and blocked with Pluronic, we elicited

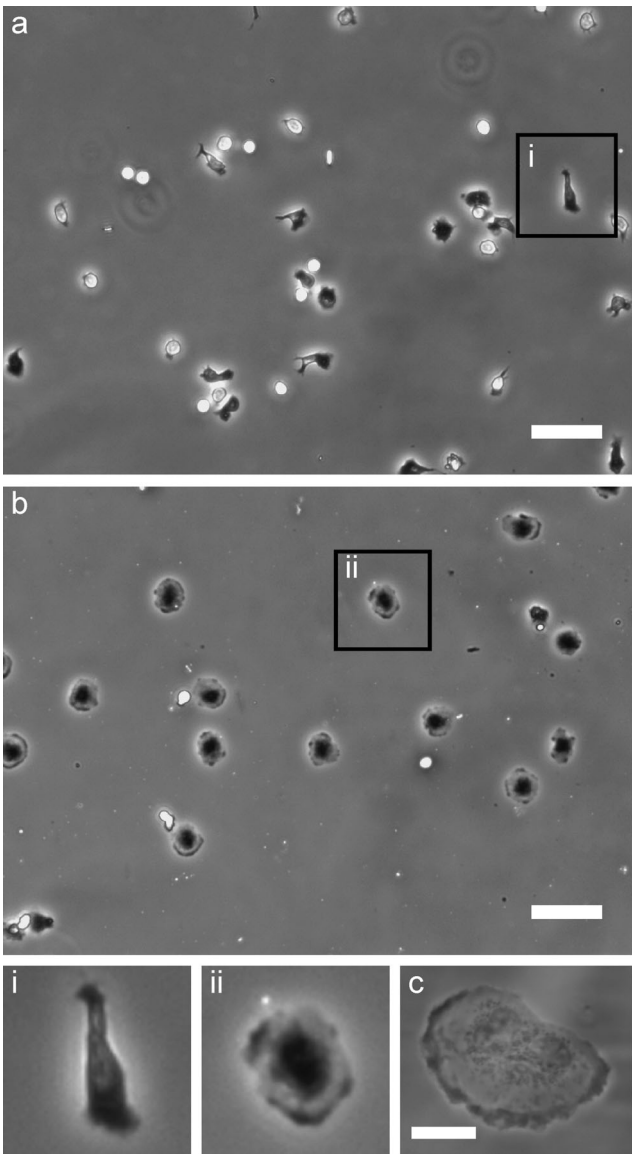

Fig. 1 Two neutrophil morphologies. (a) FN-adsorbed glass, blocked with BSA. Scalebar is 50 μm. Region (i) is enlarged 3×. (b) FN-printed PDMS, blocked with Pluronic. Scalebar is 50 μm. Region (ii) is enlarged 3×. (c) Sample cell from the same preparation as (b) but higher magnification image. Scalebar is 10 μm.

a very different phenotype. In this case, the neutrophils were well spread and no trailing uropods were discernible (Fig. 1b). With this phenotype, the cells appeared to glide and were highly persistent in their direction (Movie S2, ESI†). Our impression is that this latter phenotype was more qualitatively reminiscent of fish-keratocytes[8a] than amoeboid cells.

Complementary controls of neutrophils on FN-printed glass and FN-adsorbed PDMS demonstrated that the phenotypic differences depended on the blocking agent, not the method of protein deposition (ESI,† Fig. S1a–d). Quantitative fluorescence measurements of fluorophore-labeled FN confirmed that total FN loading of glass and PDMS surfaces were comparable (ESI,† Fig. S1e). When we silanized glass and then blocked surfaces with Pluronic, we found the well-spread, uropod-absent phenotype could be elicited on FN functionalized glass (ESI,† Fig. S2a). Our interpretation is that when blocking with Pluronic, cell binding was solely due to the underlying FN, the blocking agent did not contribute to adhesion (ESI,† Fig. S3c–e).

We hypothesized that the amoeboid phenotype is a result of adhesion to high densities of surface ligand, and that blocking with BSA served to increase the total ligand content. To test this hypothesis, we used microcontact printing to systematically control the density and type of surface ligand (ESI,† Fig. S4a). Microcontact printing is a tool to spatially pattern cellular adhesive ligands[9,12] and to print the tips of polymeric posts for force measurements.[13] While microcontact printing has been extensively used to study the behavior of mesenchymal[9,12–14] cells, it has only recently been applied in studies of hematopoietic-derived cells.[15] In our study, microcontact printing was used to immobilize different densities of FN on PDMS. By titrating the inking concentration of the protein solution used to prepare the stamps, we could reproducibly achieve sub-saturating densities of deposited FN (ESI,† Fig. S4b). After fabricating a series of PDMS surfaces with systematically varied densities of FN, all blocked with Pluronic F-127, we scored the resulting neutrophil phenotypes observed (Fig. 2a).

On surfaces printed with little or no FN and blocked with Pluronic, cells failed to polarize or spread and remained spherical, presenting as bright white circles under phase contrast imaging (Fig. 2i). On intermediate densities of printed-FN, blocked with Pluronic, the well-spread, uropod-absent phenotype was observed (Fig. 2ii). The frequency of the keratocyte-like phenotype was highest at 40% surface saturation. As the density of FN increased, the well-spread phenotype was observed less frequently. Once surface density reached 83% saturation, the amoeboid phenotype was predominate (Fig. 2iv).

Others have observed this well-spread, uropod-absent phenotype in neutrophils on FN-conjugated polyacrylamide gels.[7] In those instances, the morphology was attributed to the underlying stiffness of the material, as neutrophils on softer gels were more amoeboid. Indeed, our relatively thick PDMS layers ($\sim$12 μm) and the use of a 10 : 1 formulation (base : cure, w/w) means the substrates were quite stiff, with Young's moduli on the order of megapascals.[16] However, here we demonstrated that the well-spread phenotype on stiff surfaces is only inducible

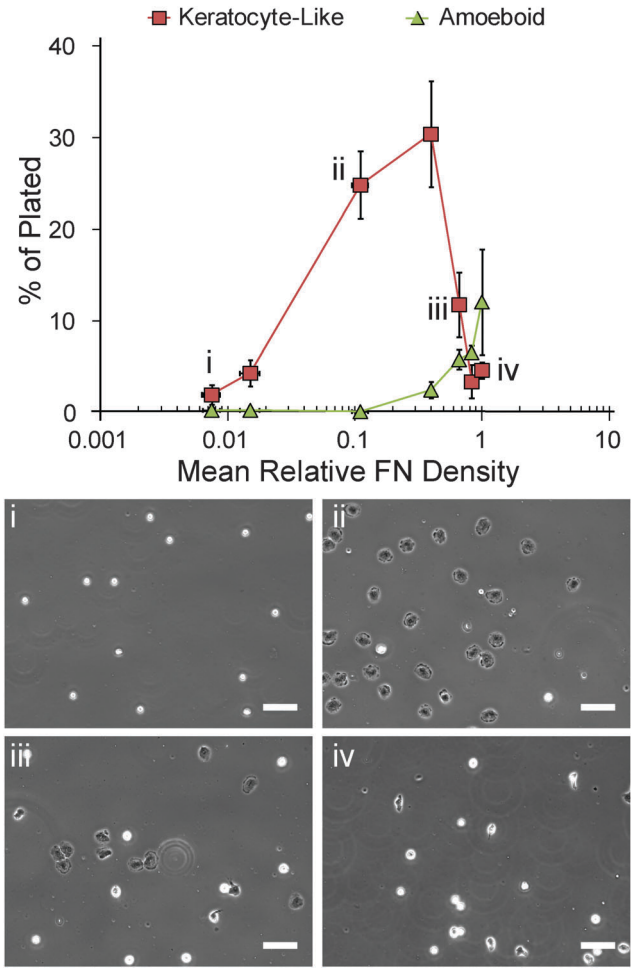

Fig. 2 Neutrophil phenotype on increasing densities of FN. Adherent neutrophils as percentage of total plated cells per FN surface density. Representative images from a single experiment on (i) 0.7% (ii) 11% (iii) 66% and (iv) 100% saturated FN substrates. Scalebars are 50 μm. Error bars are ± standard error of the mean. Substrate density was measured *via* quantitative fluorescence microscopy (ESI,† Fig. S4b). All substrates were FN-printed and Pluronic-blocked PDMS.

for sub-saturating densities of ligand. This observation contributes to the growing empirical body of evidence showing neutrophils and other leukocytes can adopt a variety of motile mechanisms to achieve translocation and helps reconcile the occurrence of both phenotypes reported elsewhere on neutrophil motility on stiff substrates.

Ziebert and Aranson have constructed a biophysical model of cell motility that demonstrates phenotypic transitions in the mode of migration as a function of underlying substrate stiffness and surface adhesivity.[8b] On stiff substrates their model predicts a transition from stick-slip to gliding motion as surface ligand density is increased. While we have not observed stick-slip motion at low adhesivity we have found that at intermediate ligand densities, neutrophils display a highly persistent gliding phenotype. It will be interesting to see if the incorporation of intracellular viscoelasticity into their future models can recapitulate our transition from gliding motion to amoeboid motion at saturating conditions of adhesive ligand. A transition

from gliding to more erratic motion has also been reported of fish keratocytes on stiff substrates as surface adhesivity increases.[8a]

Our study of how neutrophil phenotype depends on adhesion draws an interesting qualitative comparison with recent work on the capacity of physical confinement to dictate migratory cell phenotype. Migratory cells in physically confined channels or on narrow one-dimensional tracks of ligand have been shown to lose characteristics of conventional two-dimensional migration.[4c] Hung and co-workers have also found that the mechanism of propulsion differs as a function of substrate dimensionality.[17] In the future, immunocytochemical staining and small molecule inhibitor studies of our amoeboid and keratocyte-like morphologies may reveal similar discrepancies driven by ligand density.

Quantifying motility of amoeboid and keratocyte-like phenotypes

The dynamics of amoeboid and keratocyte-like motility were distinct, as revealed by comparing their mean squared displacements (MSD) as a function of time (Fig. 3). On log–log axes, the slopes of MSD *vs.* time for the two populations were different. Neutrophils undergoing amoeboid migration accumulated squared displacement diffusively (slope ~ 1) while neutrophils undergoing keratocyte-like migration accumulated squared displacement superdiffusively (slope > 1). Fitting the curves of MSD *vs.* time with the persistent random walk model of cell kinesis[18] ($\langle \mathrm{MSD}(\tau) \rangle = 2S^2P[\tau - P(1 - \exp(-\tau/P))]$) allowed us to quantify neutrophil motility in terms of the best-fit parameters speed (S) and persistence (P). Doing so confirmed our qualitative assessment that amoeboid motility was faster and less persistent (S_{amoeboid} = 6 μm min^{-1}, P_{amoeboid} = 0.5 min) than keratocyte-like motility ($S_{\mathrm{keratocyte\text{-}like}}$ = 3 μm min^{-1}, $P_{\mathrm{keratocyte\text{-}like}}$ = 15 min). Comparing the cytoskeletal architecture of these two dramatically different phenotypes remains to be done. It will be interesting to learn how stress fibers are organized in the keratocyte-like cell, compared to the amoeboid cell.

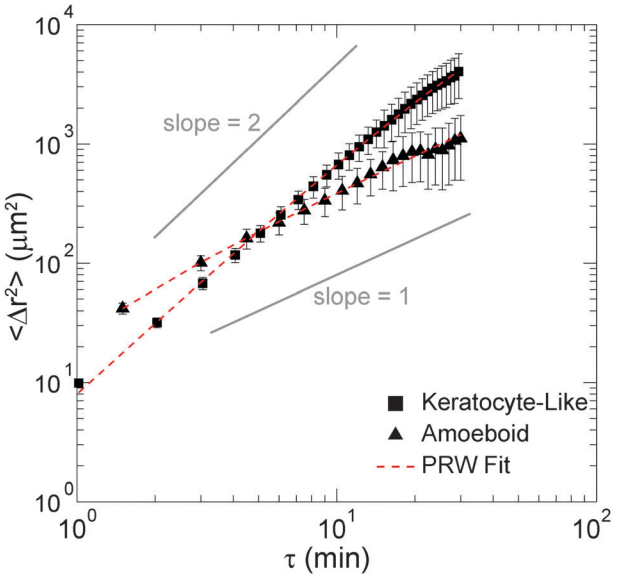

Fig. 3 Mean squared displacements (MSDs) of two motility modes. Time and ensemble averaged MSDs of neutrophils undergoing amoeboid motility or keratocyte-like motility. Amoeboid cells acquire displacement diffusively, slope ~ 1. Keratocyte-like cells acquire displacement superdiffusively, slope > 1. Dotted line is fit of empirical data with persistent random walk (PRW) model of cell motility. Error bars are ± standard error of the mean.

To this point neutrophils were induced to adhere and crawl on FN substrates without prior or concurrent stimulation by soluble chemoattractant. Therefore, the resulting motility was haptokinetic, driven by FN stimulation at the cell–substrate interface. A control study quantifying selectin-expression[19] *via* flow cytometry confirmed neutrophils were not primed for integrin-based adhesion to FN surfaces by virtue of isolation or storage stresses (ESI,† Fig. S5).

Effect of chemoattractant on keratocyte-like motility

We explored the capacity of the potent neutrophil chemoattractant formyl-Met-Leu-Phe (fMLF)[20] to modulate the motility of neutrophils undergoing keratocyte-like migration. On 44% saturated FN surfaces, the addition of 10 nM fMLF to haptokinetic neutrophils had the effect of increasing the total dispersion of the cells (Fig. 4a and b). To quantify the extent of motility in a model-independent fashion we extracted the maximum displacements for cells tracked over 30 min. Cell trajectories shorter than 30 min were excluded in this analysis to avoid inadvertently biasing the data. The mean of the maximum displacements ($\langle \max(|\Delta r|) \rangle$) was computed for each combination of FN adhesiveness and fMLF concentration (Fig. 4c). Introducing fMLF, after onset of FN-induced haptokinesis, potentiated motility in a dosage-dependent manner at an intermediate ligand density of 44% saturation. However, at a higher surface saturation of 73%, fMLF was no longer capable of increasing the basal motility induced by FN stimulation. The number of independent observations for each condition and a comprehensive description of mean maximum displacement data are reported in ESI,† Fig. S6.

Computation of the MSD provides dynamic information on the dispersion of cells and allows the incorporation of cell trajectories shorter than the total experimental acquisition time. Time and ensemble-averaged MSDs for each independent observation were computed from all available cell trajectories through 30 min. The MSDs corresponding to Fig. 4a and b data are reported in Fig. 4d. In general, on log–log axes, the slope of the MSD curves are relatively constant and greater than unity. This denotes superdiffusive motility in which cells accumulate squared displacement faster than expected by pure diffusion. Considering the best-fit parameters speed and persistence, systematic variation in the dose of fMLF alters cell speed at intermediate density FN (Fig. 4e), but not the persistence time for any of the FN-fMLF conditions tested (Fig. 4f). All MSD *vs.* time data curves contributing to construction of Fig. 4e and f are compiled in ESI,† Fig. S7 along with comparisons of data on mean speed.

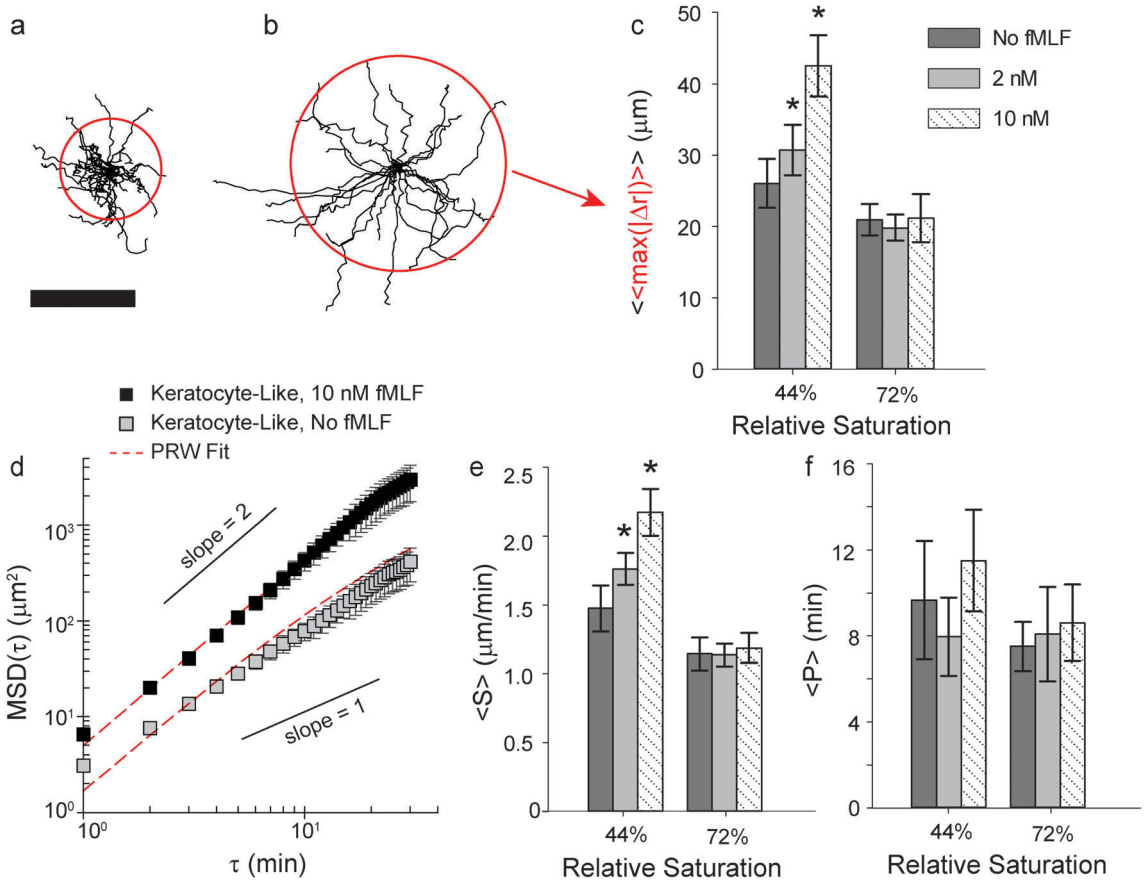

Fig. 4 Quantification of neutrophil haptokinesis and chemokinesis of keratocyte-like phenotype. Human neutrophil trajectories through 30 min of motility on 44% FN-saturated surface in (a) the absence of fMLF and (b) the presence of 10 nM fMLF. Scalebar is 50 μm. Solid red circle is the mean maximum displacement ($\langle\langle \max(|\Delta r|)\rangle\rangle$) of 30 min neutrophil trajectories for (a) $\langle \max(|\Delta r|)\rangle \sim 24$ μm and (b) $\langle \max(|\Delta r|)\rangle \sim 51$ μm. (c) Mean of the set of mean maximum displacements for all independent observations of a particular FN density and fMLF combination tested ($\langle\langle \max(|\Delta r|)\rangle\rangle$). (d) MSD($\tau$) corresponding to a single donor's neutrophils migrating on 44% FN-saturated surface in the presence or absence of fMLF. Dotted red line is fit of persistent random walk model (PRW) to empirical data. Model fit parameters (e) speed and (f) persistence. Error bars are ± standard error of the mean. Asterisk denotes significant difference relative to No fMLF condition as computed by post-hoc SNK Multiple Comparisons Method ($p < 0.05$).

In both analyses the capacity of chemoattractant to augment haptokinetic motility in the keratocyte-like phenotype was found to be a function of the underlying adhesiveness. This emphasizes the importance of considering the role of substrate adhesiveness in controlling the cell response to the milieu of soluble chemoattractants and cytokines known to orchestrate directional motility during inflammation.

Identifying integrin chains responsible for adhesion

To identify the integrin chains responsible for neutrophil binding to FN, function-blocking antibodies with previously demonstrated efficacy in leukocytes were employed.[21] Functional blocking of β_2 integrins (Fig. 5d) resulted in a substantial decrease in cell adhesion on FN relative to the positive control without antibody present (Fig. 5a). Targeting the α_M integrin, which coordinates with β_2 integrin to form the MAC-1 heterodimer, was also found to disrupt cell binding on FN significantly (Fig. 5f). In neither case did blocking β_1 (Fig. 5c) nor α_5 (Fig. 5e) integrin chains disrupt binding. These results led us to attribute the observed FN-induced adhesion and subsequent haptokinesis to the β_2 and α_M integrin subunits, or the MAC-1 receptor.

In neutrophils there is known cross talk between β_1 and β_2 integrins when ligating extracellular matrix proteins such as FN.[21a,22] Our finding that neutrophils utilize MAC-1 ($\alpha_M\beta_2$) on FN is consistent with other empirical observations. In particular van den Berg and coworkers demonstrated that stimulation of β_1 integrins yields β_2-mediated adhesion in neutrophils on FN that can be mitigated by function-blocking antibodies against MAC-1.[21a] Our blocking study is a probe on the long time-limit (*i.e.* minute length scale) adhesion of neutrophils to FN. Lishko and co-workers demonstrated that a balance of MAC-1 and VLA-5 ($\alpha_5\beta_1$) is required for neutrophil translocation on FN attributing MAC-1 to adhesion and VLA-5 to migration.[22] Our work reveals that MAC-1 is the dominant ligated integrin and may explain the reduced speed of the keratocyte-like phenotype.

MAC-1 also binds to members of the Ig superfamily,[23] such as ICAM-1, which illustrates the promiscuity of this integrin. We hypothesized that the emergence of the amoeboid phenotype on BSA-blocked surfaces of intermediate density FN was due to

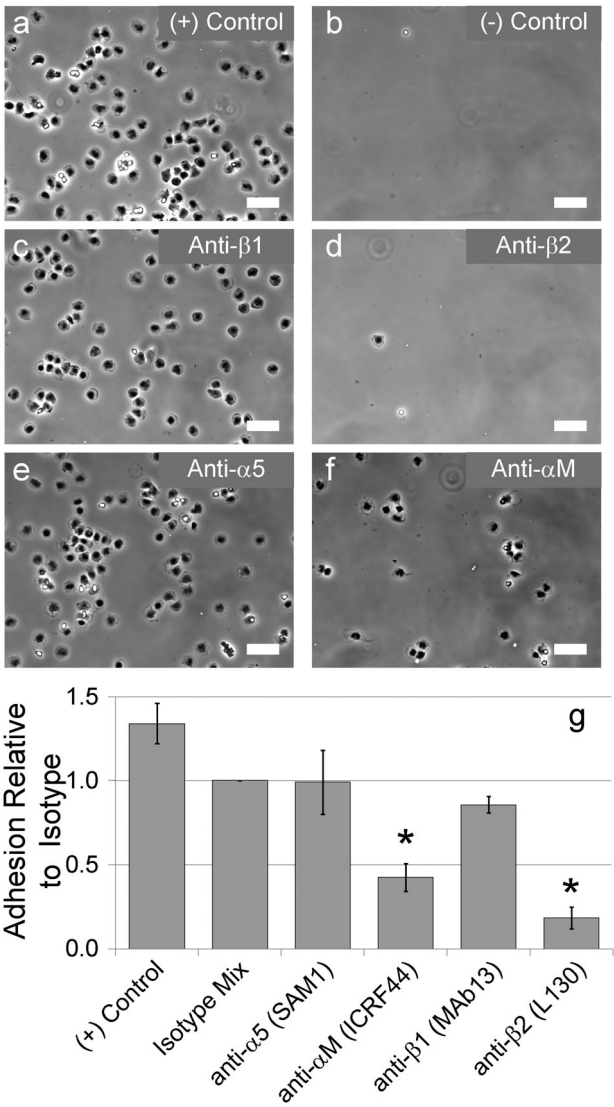

Fig. 5 Integrin blocking on FN. Integrin blocking of neutrophils pre-incubated with antibodies against various integrin chains before exposure to 44% FN-saturated surface. (a) Positive binding control, no antibodies. (b) Negative binding control, no FN, just Pluronic blocking. (c) anti-β_1 clone MAb13, (d) anti-β_2 clone L130, (e) anti-α_5 clone SAM1, and (f) anti-α_M clone ICRF44. Scalebars are 50 μm. (g) Mean ratio of adherent cells to isotype control. Error bars are ± standard error of the mean (n = 3–4). Asterisk denotes significant difference relative to isotype control as computed by post-hoc Dunnet's Method ($p < 0.05$).

simultaneous binding of MAC-1 to BSA and FN. Indeed, we were able to recapitulate the keratocyte-like phenotype on intermediate densities of BSA alone (Fig. 6a). The percentage of plated neutrophils exhibiting keratocyte-like phenotype on fields of BSA at sub-saturating density was 63% (n = 3, SE = 22%). Furthermore, at saturating densities of BSA alone, neutrophils again switched to the amoeboid phenotype (Fig. 6b). The percentage of plated neutrophils exhibiting amoeboid phenotype on fields of BSA at saturating density was 73% (n = 1, SD = 4%). When we repeated the function-blocking antibody study on neutrophils exposed to intermediate-density BSA substrates, we again found that MAC-1 was mediating adhesion (Fig. 6c).

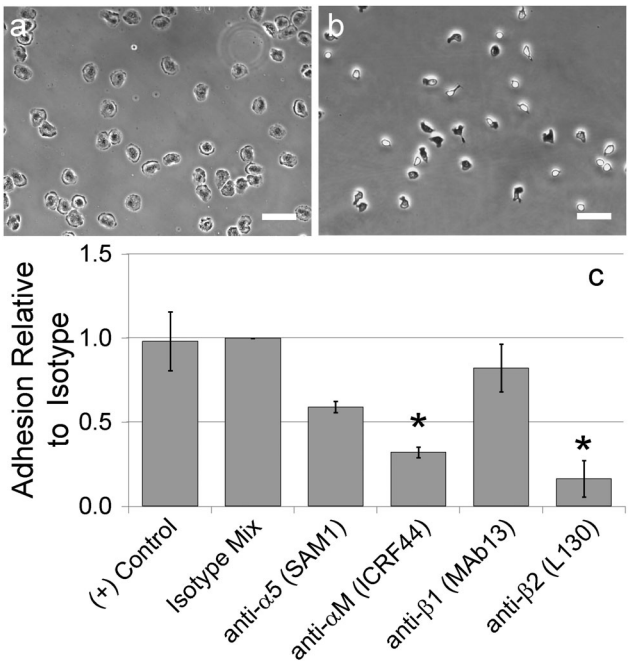

Fig. 6 Neutrophil adhesion to BSA. (a) Keratocyte-like phenotype of neutrophils on intermediate density of BSA. (b) Amoeboid phenotype returns on saturating density of BSA. (c) Recapitulation of antibody blocking study of neutrophils on intermediate density BSA surfaces. Mean ratio of adherent cells to isotype control. Error bars are ± standard error of the mean (n = 2–3). Asterisk denotes significant difference relative to isotype control as computed by post-hoc Dunnet's Method ($p < 0.05$).

The finding that neutrophils were employing the promiscuous integrin MAC-1 to mediate adhesion to our experimental surfaces reinforces the necessity of choosing an appropriate blocking reagent against non-specific cell adhesion. BSA, which is often used to block surfaces, actually functions as an adhesive ligand. Coating surfaces with Pluronic is the only method we have found to reliably eliminate all non-specific background adhesion in our *in vitro* motility assays. This type of exquisite discrimination of the roles of different ligands is only possible with improved surface techniques, such as microcontact printing.[9]

Aside from the obvious conclusion that care must be taken to block non-specific binding with appropriately neutral ligands, future work will address how the organization and density of adhesion ligands leads to the morphology of cell response. Now, we can speculate that a high density of adhesion ligands over a large spatial domain promotes uropod formation. If this is the case, distribution of ligands into patches would prevent uropod formation, even if the density in the patches were locally high.

Conclusions

Our work has demonstrated that neutrophils are capable of a phenotypic switch in morphology and associated motility as dictated by adhesion ligand density. The nature of the density sensing remains to be addressed in determining whether

neutrophils are sensitive to these changes at the receptor length scale or across their total cell–substrate contact area. We anticipate microcontact printing will be a useful platform in addressing this question. By quantifying the motility associated with the amoeboid and keratocyte-like phenotypes we found the modes of migration to be distinct. The biophysical mechanism that underpins these differences is unclear. We suspect visualizing cytoskeletal architectures will improve our mechanistic insight. Lastly, our finding that the integrin heterodimer MAC-1 was being employed to mediate adhesion to our experimental surfaces reinforces the importance of avoiding BSA as an agent to block non-specific binding in neutrophils.

Acknowledgements

We are grateful to Eric Johnston for technical assistance in the laboratory and Drs Christopher S. Chen, Michael T. Yang and Ravi A. Desai for their time and expertise in teaching us microcontact printing. Funding for this work was provided by a National Science Foundation Graduate Research Fellowship to SJH and a grant from the National Institutes of Health (HL18208) to DAH.

References

1 C. Nathan, Neutrophils and immunity: challenges and opportunities, *Nat. Rev. Immunol.*, 2006, **6**, 173–182, DOI: 10.1038/nri1785.

2 B. McDonald, K. Pittman, G. B. Menezes, S. A. Hirota, I. Slaba, C. C. M. Waterhouse, P. L. Beck, D. A. Muruve and P. Kubes, Intravascular Danger Signals Guide Neutrophils to Sites of Sterile Inflammation, *Science*, 2010, **330**, 362–366, DOI: 10.1126/science.1195491.

3 (*a*) D. Irimia, S.-Y. Liu, W. G. Tharp, A. Samadani, M. Toner and M. C. Poznansky, Microfluidic system for measuring neutrophil migratory responses to fast switches of chemical gradients, *Lab Chip*, 2006, **6**, 191–198, DOI: 10.1039/b511877h; (*b*) E. K. Sackmann, E. Berthier, E. W. K. Young, M. A. Shelef, S. A. Wernimont, A. Huttenlocher and D. J. Beebe, Microfluidic kit-on-a-lid: a versatile platform for neutrophil chemotaxis assays, *Blood*, 2012, **120**, e45–e53, DOI: 10.1182/blood-2012-03-416453.

4 (*a*) T. Lammermann, B. L. Bader, S. J. Monkley, T. Worbs, R. Wedlich-Soldner, K. Hirsch, M. Keller, R. Forster, D. R. Critchley, R. Fassler and M. Sixt, Rapid leukocyte migration by integrin-independent flowing and squeezing, *Nature*, 2008, **453**, 51–55, DOI: 10.1038/nature06887; (*b*) R. J. Hawkins, M. Piel, G. Faure-Andre, A. M. Lennon-Dumenil, J. F. Joanny, J. Prost and R. Voituriez, Pushing off the Walls: A Mechanism of Cell Motility in Confinement, *Phys. Rev. Lett.*, 2009, **102**, 058103, DOI: 10.1103/PhysRevLett.102.058103; (*c*) K. Konstantopoulos, P.-H. Wu and D. Wirtz, Dimensional Control of Cancer Cell Migration, *Biophys. J.*, 2013, **104**, 279–280, DOI: 10.1016/j.bpj.2012.12.016.

5 (*a*) S. H. Zigmond, Chemotaxis by polymorphonuclear leukocytes, *J. Cell Biol.*, 1978, **77**, 269–287; (*b*) S. E. Malawista and A. d. B. Chevance, Random locomotion and chemotaxis of human blood polymorphonuclear leukocytes (PMN) in the presence of EDTA: PMN in close quarters require neither leukocyte integrins nor external divalent cations, *Proc. Natl. Acad. Sci. U. S. A.*, 1997, **94**, 11577–11582; (*c*) L. M. Butler, S. Khan, G. Ed Rainger and G. B. Nash, Effects of endothelial basement membrane on neutrophil adhesion and migration, *Cell. Immunol.*, 2008, **251**, 56–61, DOI: 10.1016/j.cellimm.2008.04.004; (*d*) A. R. Houk, A. Jilkine, C. O. Mejean, R. Boltyanskiy, E. R. Dufresne, S. B. Angenent, S. J. Altschuler, L. F. Wu and O. D. Weiner, Membrane Tension Maintains Cell Polarity by Confining Signals to the Leading Edge during Neutrophil Migration, *Cell*, 2012, **148**, 175–188, DOI: 10.1016/j.cell.2011.10.050; (*e*) M. Yanai, J. P. Butler, T. Suzuki, H. Sasaki and H. Higuchi, Regional rheological differences in locomoting neutrophils, *Am. J. Physiol.: Cell Physiol.*, 2004, **287**, C603–C611, DOI: 10.1152/ajpcell.00347.2003.

6 (*a*) L. Cassimeris, H. McNeill and S. H. Zigmond, Chemoattractant-stimulated polymorphonuclear leukocytes contain two populations of actin filaments that differ in their spatial distributions and relative stabilities, *J. Cell Biol.*, 1990, **110**, 1067–1075, DOI: 10.1083/jcb.110.4.1067; (*b*) Y. Matzner, I. Vlodavsky, R. I. Michaeli and A. Eldor, Selective inhibition of neutrophil activation by the subendothelial extracellular matrix: possible role in protection of the vessel wall during diapedesis, *Exp. Cell Res.*, 1990, **189**, 233–240.

7 (*a*) P. W. Oakes, D. C. Patel, N. A. Morin, D. P. Zitterbart, B. Fabry, J. S. Reichner and J. X. Tang, Neutrophil morphology and migration are affected by substrate elasticity, *Blood*, 2009, **114**, 1387–1395, DOI: 10.1182/blood-2008-11-191445; (*b*) K. M. Stroka and H. Aranda-Espinoza, Neutrophils display biphasic relationship between migration and substrate stiffness, *Cell Motil. Cytoskeleton*, 2009, **66**, 328–341, DOI: 10.1002/cm.20363; (*c*) R. A. Jannat, G. P. Robbins, B. G. Ricart, M. Dembo and D. A. Hammer, Neutrophil adhesion and chemotaxis depend on substrate mechanics, *J. Phys.: Condens. Matter*, 2010, **22**, 194117, DOI: 10.1088/0953-8984/22/19/194117.

8 (*a*) E. L. Barnhart, K. C. Lee, K. Keren, A. Mogilner and J. A. Theriot, An adhesion-dependent switch between mechanisms that determine motile cell shape, *PLoS Biol.*, 2011, **9**, e1001059, DOI: 10.1371/journal.pbio.1001059; (*b*) F. Ziebert and I. S. Aranson, Effects of adhesion dynamics and substrate compliance on the shape and motility of crawling cells, *PLoS One*, 2013, **8**, e64511, DOI: 10.1371/journal.pone.0064511.

9 R. A. Desai, M. K. Khan, S. B. Gopal and C. S. Chen, Subcellular spatial segregation of integrin subtypes by patterned multicomponent surfaces, *Integr. Biol.*, 2011, **3**, 560–567, DOI: 10.1039/c0ib00129e.

10 J. L. Tan, W. Liu, C. M. Nelson, S. Raghavan and C. S. Chen, Simple approach to micropattern cells on common culture

substrates by tuning substrate wettability, *Tissue Eng.*, 2004, **10**, 865–872, DOI: 10.1089/1076327041348365.

11 J. C. Crocker and B. D. Hoffman, Multiple-particle tracking and two-point microrheology in cells, *Methods Cell Biol.*, 2007, **83**, 141–178, DOI: 10.1016/S0091-679x(07)83007-X.

12 C. S. Chen, M. Mrksich, S. Huang, G. M. Whitesides and D. E. Ingber, Geometric control of cell life and death, *Science*, 1997, **276**, 1425–1428, DOI: 10.1126/science.276.5317.1425.

13 J. L. Tan, J. Tien, D. M. Pirone, D. S. Gray, K. Bhadriraju and C. S. Chen, Cells lying on a bed of microneedles: An approach to isolate mechanical force, *Proc. Natl. Acad. Sci. U. S. A.*, 2003, **100**, 1484–1489, DOI: 10.1073/pnas.0235407100.

14 (*a*) M. Thery, V. Racine, A. Pepin, M. Piel, Y. Chen, J.-B. Sibarita and M. Bornens, The extracellular matrix guides the orientation of the cell division axis, *Nat. Cell Biol.*, 2005, **7**, 947–953, DOI: 10.1038/ncb1307; (*b*) S. Y. Tee, J. Fu, C. S. Chen and P. A. Janmey, Cell shape and substrate rigidity both regulate cell stiffness, *Biophys. J.*, 2011, **100**, L25–L27, DOI: 10.1016/j.bpj.2010.12.3744; (*c*) S. A. Ruiz and C. S. Chen, Microcontact printing: A tool to pattern, *Soft Matter*, 2007, **3**, 168–177, DOI: 10.1039/b613349e.

15 (*a*) D. Lee and M. R. King, Microcontact printing of P-selectin increases the rate of neutrophil recruitment under shear flow, *Biotechnol. Prog.*, 2008, **24**, 1052–1059, DOI: 10.1002/btpr.35; (*b*) B. G. Ricart, M. T. Yang, C. A. Hunter, C. S. Chen and D. A. Hammer, Measuring traction forces of motile dendritic cells on micropost arrays, *Biophys. J.*, 2011, **101**, 2620–2628, DOI: 10.1016/j.bpj.2011.09.022; (*c*) K. Shen, V. K. Thomas, M. L. Dustin and L. C. Kam, Micropatterning of costimulatory ligands enhances CD4 + T cell function, *Proc. Natl. Acad. Sci. U. S. A.*, 2008, **105**, 7791–7796, DOI: 10.1073/pnas.0710295105; (*d*) Z. Tong, L. S. Cheung, K. J. Stebe and K. Konstantopoulos, Selectin-mediated adhesion in shear flow using micropatterned substrates: multiple-bond interactions govern the critical length for cell binding, *Integr. Biol.*, 2012, **4**, 847–856, DOI: 10.1039/c2ib20036h.

16 (*a*) X. Q. Brown, K. Ookawa and J. Y. Wong, Evaluation of polydimethylsiloxane scaffolds with physiologically-relevant elastic moduli: interplay of substrate mechanics and surface chemistry effects on vascular smooth muscle cell response, *Biomaterials*, 2005, **26**, 3123–3129, DOI: 10.1016/j.biomaterials.2004.08.009; (*b*) D. Fuard, T. Tzvetkova-Chevolleau, S. Decossas, P. Tracqui and P. Schiavone, Optimization of poly-di-methyl-siloxane (PDMS) substrates for studying cellular adhesion and motility, *Microelectron. Eng.*, 2008, **85**, 1289–1293, DOI: 10.1016/j.mee.2008.02.004.

17 W.-C. Hung, S.-H. Chen, C. D. Paul, K. M. Stroka, Y.-C. Lo, J. T. Yang and K. Konstantopoulos, Distinct signaling mechanisms regulate migration in unconfined *versus* confined spaces, *J. Cell Biol.*, 2013, **202**, 807–824, DOI: 10.1083/jcb.201302132.

18 (*a*) G. A. Dunn, Characterising a kinesis response: time averaged measures of cell speed and directional persistence, *Agents Actions Suppl.*, 1983, **12**, 14–33; (*b*) D. A. Lauffenburger and J. J. Linderman, *Receptors: models for binding, trafficking, and signaling*, Oxford University Press, New York, 1993, p. 365.

19 T. K. Kishimoto, M. A. Jutila, E. L. Berg and E. C. Butcher, Neutrophil Mac-1 and MEL-14 adhesion proteins inversely regulated by chemotactic factors, *Science*, 1989, **245**, 1238–1241, DOI: 10.1126/science.2551036.

20 E. Schiffmann, B. A. Corcoran and S. M. Wahl, N-formylmethionyl peptides as chemoattractants for leucocytes, *Proc. Natl. Acad. Sci. U. S. A.*, 1975, **72**, 1059–1062.

21 (*a*) J. M. van den Berg, F. P. Mul, E. Schippers, J. J. Weening, D. Roos and T. W. Kuijpers, Beta1 integrin activation on human neutrophils promotes beta2 integrin-mediated adhesion to fibronectin, *Eur. J. Immunol.*, 2001, **31**, 276–284, DOI: 10.1002/1521-4141(200101)31:1<276::AID-IMMU276>3.0.CO;2-D; (*b*) T. W. Penberthy, Y. Jiang, F. W. Luscinskas and D. T. Graves, MCP-1-stimulated monocytes preferentially utilize beta 2-integrins to migrate on laminin and fibronectin, *Am. J. Physiol.*, 1995, **269**, C60–C68.

22 V. K. Lishko, V. P. Yakubenko and T. P. Ugarova, The interplay between integrins alphaMbeta2 and alpha5beta1 during cell migration to fibronectin, *Exp. Cell Res.*, 2003, **283**, 116–126, DOI: 10.1016/S0014-4827(02)00024-1.

23 (*a*) R. B. Henderson, L. H. Lim, P. A. Tessier, F. N. Gavins, M. Mathies, M. Perretti and N. Hogg, The use of lymphocyte function-associated antigen (LFA)-1-deficient mice to determine the role of LFA-1, Mac-1, and alpha4 integrin in the inflammatory response of neutrophils, *J. Exp. Med.*, 2001, **194**, 219–226, DOI: 10.1084/jem.194.2.219; (*b*) M. Phillipson, B. Heit, P. Colarusso, L. Liu, C. M. Ballantyne and P. Kubes, Intraluminal crawling of neutrophils to emigration sites: a molecularly distinct process from adhesion in the recruitment cascade, *J. Exp. Med.*, 2006, **203**, 2569–2575, DOI: 10.1084/jem.20060925.

Electronic Supplementary Material (ESI) for Integrative Biology

Supplementary Materials

Ligand density elicits phenotypic switch in human neutrophils

Steven J. Henry, John C. Crocker, and Daniel A. Hammer

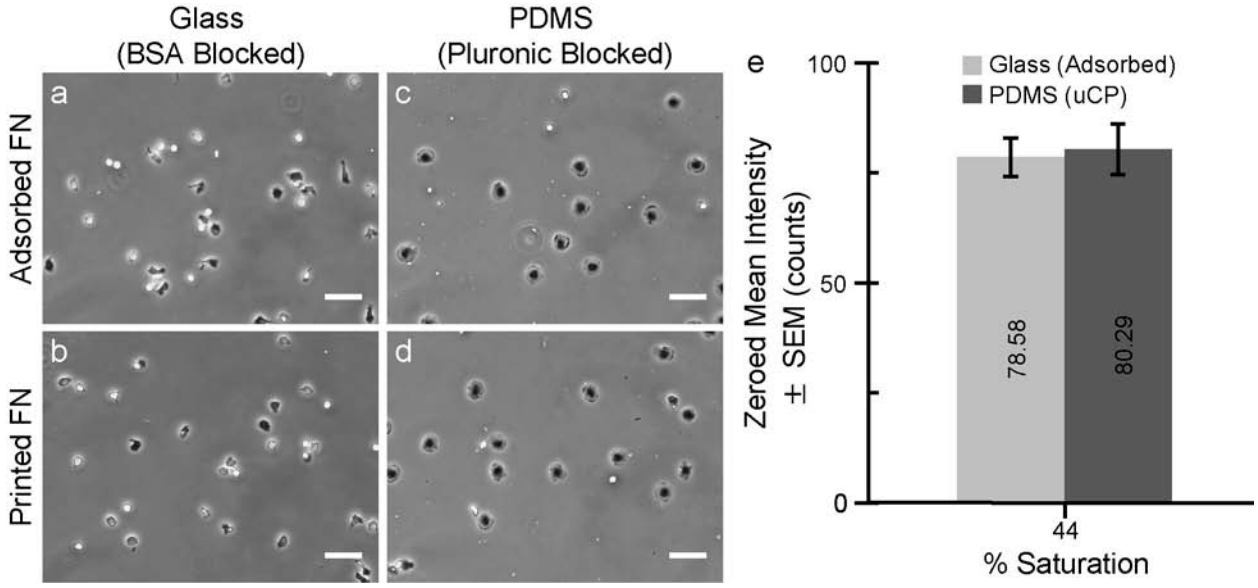

Supplementary Fig. 1 Phenotype does not follow method of protein deposition. To determine if method of protein deposition dictated the two cell phenotypes we compared the following surface preparation strategies: (a) FN-adsorbed glass, BSA blocked (reproduced from Fig. 1a of main text), (b) FN-printed glass, BSA blocked, (c) FN-adsorbed PDMS, Pluronic blocked, and (d) FN-printed PDMS, Pluronic blocked (reproduced from Fig. 1b of main text). Scalebars = 50 μm. Phenotype followed the method of blocking not the method of FN deposition. (e) Mean intensity of FN594 (FN conjugated to Alexa Fluor 594 dye) adsorbed onto glass and printed onto PDMS. Images were acquired under identical settings and the mean pixel intensity computed. For each preparation, the mean pixel intensity of the corresponding negative control was subtracted to produce the "zeroed mean intensity". Error bars are ± standard error of the mean (n = 2 independent experiments). Amount of deposited FN on both surfaces is comparable.

Electronic Supplementary Material (ESI) for Integrative Biology

Supplementary Materials

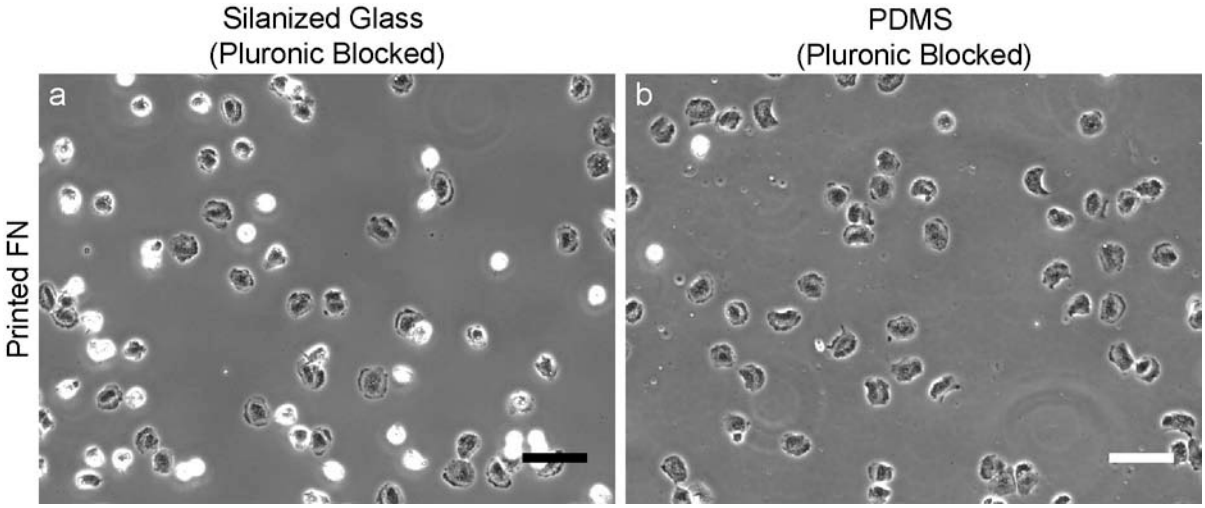

Supplementary Fig. 2 Keratocyte-like phenotype recapitulated on Pluornic-blocked glass. To determine if substrate type (i.e. glass vs. PDMS) dictated the two cell phenotypes we performed the following controls: (a) FN-printed silanized glass, Pluronic blocked (b) FN-printed PDMS, Pluronic blocked. Surfaces functionalized at 40% FN-surface saturation. Scalebars = 50 μm.

Supplementary Materials

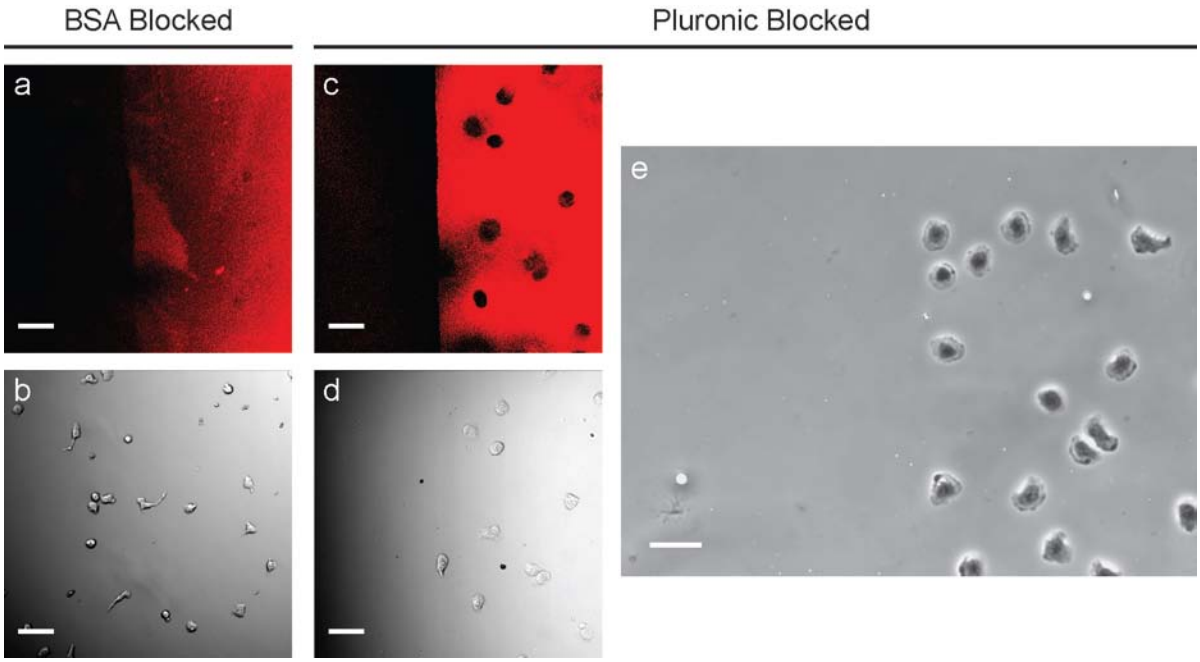

Supplementary Fig. 3 Exquisite cell-ligand specificity on Pluronic blocked substrates. Pluronic F-127 blocking of PDMS substrates allows complete inhibition of non-specific binding in human neutrophils. (a) FN conjugated to Alexa Fluor 647 (FN647) after adsorption to a piranha cleaned coverslip, blocked with 0.2% BSA in PBS (w/v). The distinct edge shown was achieved by affixing a single-well flexiPERM gasket to the coverslip which was removed prior to blocking and cell plating. (b) DIC image of fixed human neutrophils in same location as (a). Observe that cell adhesion is seen in regions of the substrate not functionalized with FN. (c) FN647 after printing on a PDMS spin-coated coverslip, blocked with 0.2% Pluronic F-127 in PBS (w/v). (d) DIC image of fixed human neutrophils on microcontact printed substrate in same location as (c). No adhesion outside of the functionalized area is observed. (e) Phase contrast image of fixed cells at a different edge location on same substrate (c-d). All scale bars are 40 μm. Note: non-uniform image acquisition parameters preclude comparison of fluorescent signal intensities between the glass and PDMS conditions (a, c). Surfaces functionalized at 40% FN surface saturation.

Supplementary Materials

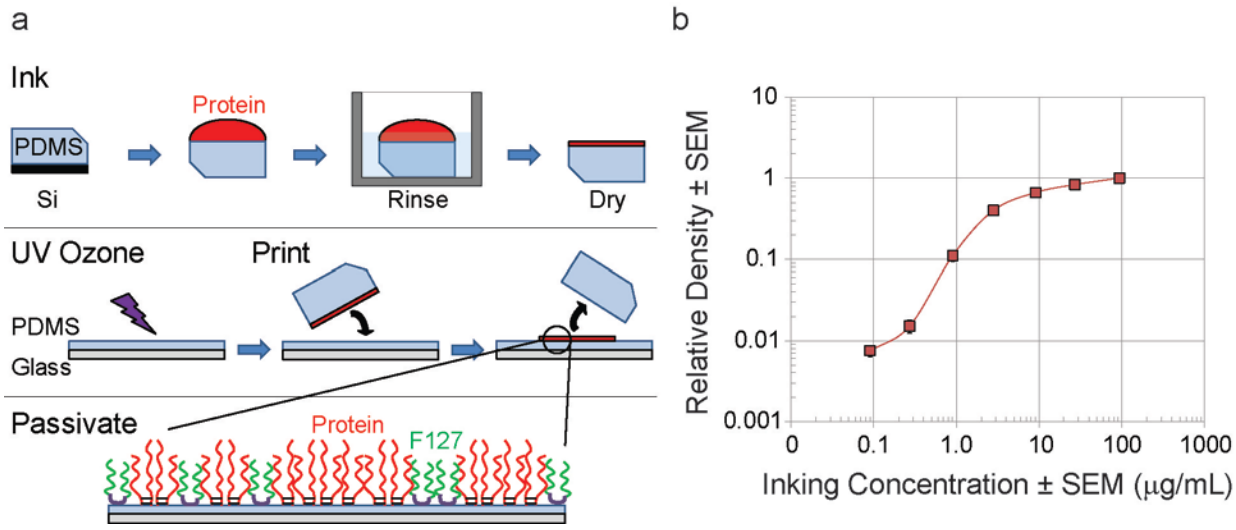

Supplementary Fig. 4 Microcontact printing overview and sub-saturating density quantification. (a) PDMS is cast against a silicon wafer to generate a smooth inking face. Stamps are trimmed and a sessile drop of protein solution at known concentration is used to coat the smooth stamping face. Stamps are rinsed and dried gently in a stream of nitrogen. Separately PDMS-spun coverslips are rendered hydrophilic by exposure to UV ozone for 7 min. When the inked stamps are brought into contact with the spun coverslip there is preferential transfer of the protein from the natively hydrophobic stamp to the hydrophilic coverslip. Finally the substrate is passivated by submersion in a nonionic triblock copolymer sold under the tradename Pluronic F127. Bare regions of the PDMS not occupied by adhesive ligand are rendered stealth to neutrophils by Pluronic coating. (b) Quantitative fluorescence microscopy to determine the relative density of protein on printed substrates by titrating inking concentration. The saturating condition was considered to be 100 μg/mL. Error bars are standard error of the mean (n = 7-9 independent experiments).

Electronic Supplementary Material (ESI) for Integrative Biology

Supplementary Materials

Flow Cytometry to Assess Activation State

Because neutrophils were robustly haptokinetic on FN alone without the addition of chemoattractant, we verified that cells were not primed for binding to the adhesion ligand as a result of stresses experienced prior to FN exposure. We used L-selectin as the marker of cell activation state. Kishimoto and coworkers demonstrated that L-selectin is a sensitive marker of a neutrophil's transition from quiescence to a phenotype primed for integrin-mediated binding [1], a transition denoted by rapid L-selectin shedding.

Staining of all treatment conditions was for 45 min on ice in the dark immediately followed by fixation in 2% formaldehyde for 20 min. After fixation, vials were spun to pellet cells (350 xg, 5 min, 4ºC) and resuspended in HBSS without calcium or magnesium. This rinsing sequence was repeated three times. After the final resuspension, cells were stored overnight on ice in the dark until flow cytometry measurements the following day. Antibodies were mouse-anti-human CD62L-PE-Cy5 (eBioscience) and mouse IgG1κ-PE-Cy5 isotype control (eBioscience).

Immediately after isolation, neutrophils were stained for L-selectin (Supplementary Fig. 5a). Positive (i.e. activated) controls were generated by exposing isolated neutrophils to the chemoattractants TNFα and fMLF immediately following isolation (Supplementary Fig. 5b,c). A decrease in L-selectin expression by cells exposed to chemoattractant, relative to the post-isolation control, demonstrated the isolated neutrophils had the capacity to be activated. To mimic the conditions cells would experience prior to plating on a FN-printed PDMS substrate, a separate aliquot of cells was subjected to storage, buffer exchange, and re-warming consistent with the plating protocol used in our motility studies. Flow cytometry on these pre-FN mimics

Supplementary Materials

(Supplementary Fig. 5d) showed a slight increase in L-selectin expression relative to the post-isolation control.

To quantify the extent of these shifts, the relative median fluorescence intensity (Relative M.F.I. = $(M.F.I._{Isotype} - M.F.I._{Sample})/M.F.I._{Isotype}$) of each condition was computed (Supplementary Fig. 5e). A statistically significant decrease in L-selectin expression as a function of TNFα was observed relative to the post-isolation control and pre-FN mimic. No statistically significant difference was found between the post-isolation control and pre-FN condition. Thus while the isolated neutrophils were capable of activation, they were not primed for integrin-mediated binding by virtue of isolation or storage stresses prior to FN exposure. This finding, coupled with high cell-FN specificity on Plurnoic blocked PDMS substrates, leads us to attribute the post-plating adhesion and haptokinesis solely to the deposited FN.

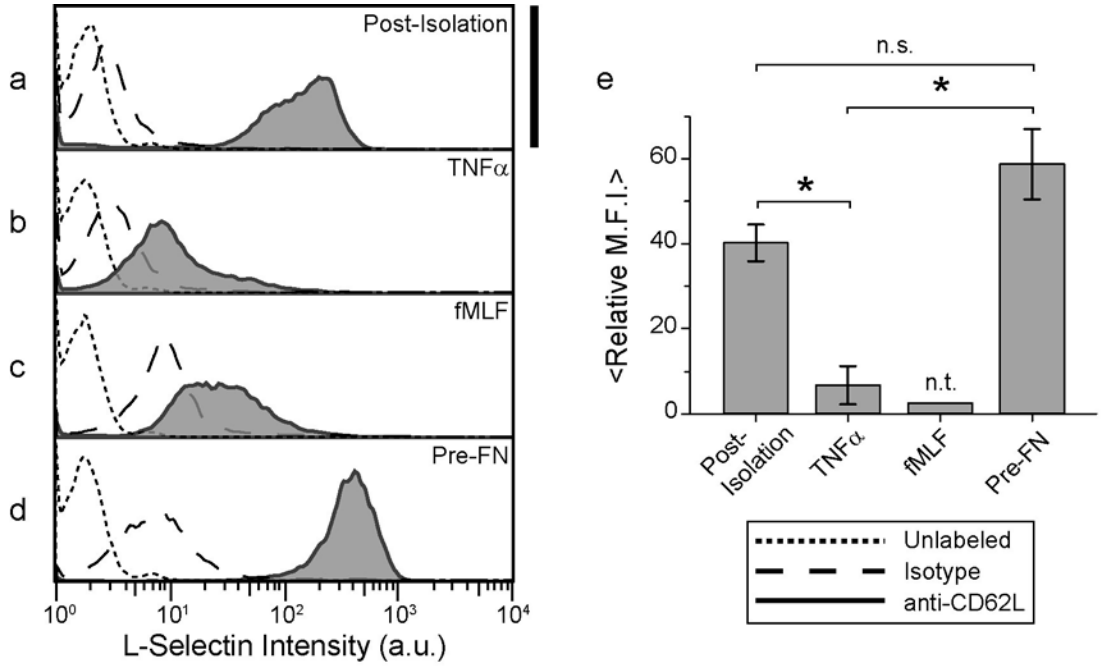

Supplementary Fig. 5 Quantification of L-selectin expression levels via flow cytometry. Expression levels were assayed under the following conditions: (a) immediately after isolation from whole blood, (b) immediately after isolation including 100 U/mL TNFα or (c) 100 nM fMLF as positive activation controls, and (d) prior to FN exposure mimicking the storage, buffer exchange, and re-warming steps experienced by plated cells. Scalebar is 400 counts. Mean relative median fluorescence intensity (Relative M.F.I) was computed for each experimental

condition (e). Errorbars are standard error of the mean (n = 2 donors). Asterisk denotes significant difference and n.s. denotes a difference not statistically significant as computed by post-hoc SNK Multiple Comparisons Method ($p < 0.05$). fMLF was excluded from significance testing (n.t.).

Supplementary Materials

a

FN	fMLF	N_{indep}	$n_{cells,tot}$	$\langle n_{cells} \rangle$	$\langle n_{cells,eff} \rangle$	$N_{indep,eff}$
% Sat.	nM	counts	counts	counts	counts	counts
44	0	8	241	30	36	6.63
44	2	6	215	36	42	5.17
44	10	7	187	27	28	6.65
72	0	7	229	33	36	6.31
72	2	5	211	42	48	4.37
72	10	5	121	24	25	4.86

b

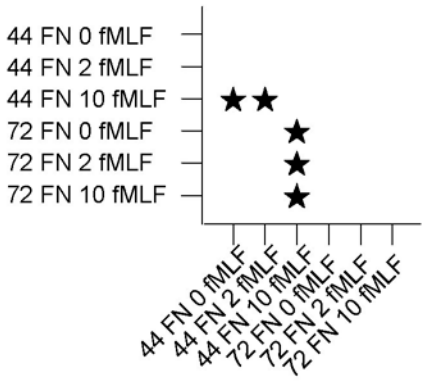

Supplementary Fig. 6 Table of sample sizes per condition and complete results of model-independent significance testing. (a) Table summarizing sample sizes for each experimental condition (FN/fMLF combination). N_{indep} (column 3) is the number of independent observations where an independent observation is a unique donor/donation combination. $N_{cells,tot}$ (column 4) is the number of total cell trajectories acquired across all independent observations. $\langle n_{cells} \rangle$ (column 5) is the average number of cells contributed by each independent observation without weighting. Because each independent observation of a condition contributed a different number of cells, weighting is required. Weighting mean values by the number of cells used in the computation of the mean results in an effective number of independent observations on the mean given by $N_{indep,eff}$ (column 7) and a corresponding effective average number of cells per independent observation $\langle n_{cells,eff} \rangle$ (column 6). These later two values can be thought of as a hypothetical number of independent observations ($N_{indep,eff}$) of equal statistical power, each experiment contributing the same number of cells ($\langle n_{cells,eff} \rangle$). (b) Complete results of significance testing corresponding to the mean maximum displacement metric of Fig. 4c in the main text. A star denotes a significance difference as computed by post-hoc SNK Multiple Comparisons Method ($p < 0.05$).

Supplementary Materials

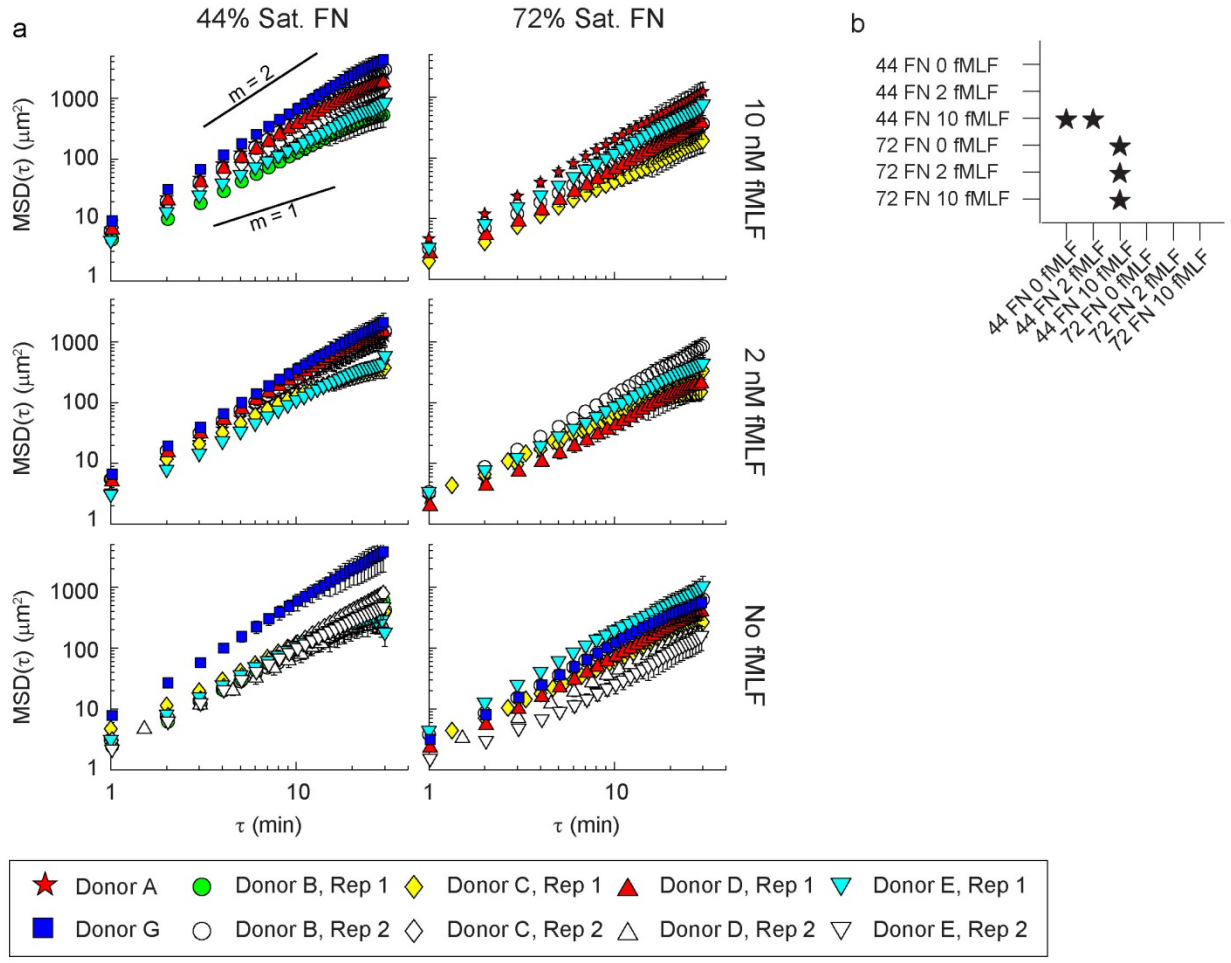

Supplementary Fig. 7 MSDs of all independent observations of FN/fMLF experimental conditions tested. (a) For a given elapsed time interval (τ), MSD(τ) is the variance of the population of displacements within and across all cells (i.e. time and ensemble averaged). τ_{min} is the experimental frame rate and τ_{max} is 30 min. This study utilized six donors (closed symbols), four of which donated on a separate experimental day (open symbols). Variability within a given donor on different experimental days for the same experimental condition led us to treat each donor/donation as an independent observation. Plots are organized by adhesiveness (columns) and concentration of fMLF (rows). All plots are scaled identically. Error bars are ± standard error of the variance (i.e. of the MSD(τ)). Eye guides of slope ("m") 1 and 2 are provided for reference. (b) Complete results of significance testing corresponding to the speed parameter "S" from the persistent random walk fit to the empirical MSDs. A star denotes a significance difference as computed by post-hoc SNK Multiple Comparisons Method ($p < 0.05$). No statistically significant differences were found among persistence values of Fig. 4e.

Supplementary Materials

Supplementary Movie S1 Amoeboid phenotype. Human neutrophil haptokinesis on 44% surface-saturated FN, adsorbed to glass, blocked with BSA.

Supplementary Movie S2 Keratocyte-like phenotype. Human neutrophil haptokinesis on 44% surface-saturated FN, printed PDMS, blocked with Pluronic F-127. Neutrophils are from same donation as Movie 1.

References:

1. T. K. Kishimoto, M. A. Jutila, E. L. Berg, E. C. Butcher, Neutrophil Mac-1 and MEL-14 adhesion proteins inversely regulated by chemotactic factors. *Science* 1989, *245*. 1238-41, DOI: 10.1126/science.2551036.